Nuclear Engineering and Design 340 (2018) 240–244

Contents lists available at ScienceDirect

Nuclear Engineering and Design

journal homepage: www.elsevier.com/locate/nucengdes

Helium solubility in oxide nuclear fuel: Derivation of new correlations for Henry's constant

ARTICLE INFO

Keywords:
Helium behaviour
Solubility
Henry's constant
Oxide fuel

ABSTRACT

Helium plays an important role in determining nuclear fuel performance both in-pile (especially for MOX fuels and those at high burnup) and in storage conditions. Predictive models of helium behaviour are therefore a fundamental element in fuel performance codes. These models are based on the accurate knowledge of helium diffusivity (addressed in a previous paper, Luzzi et al. (2018)) and of helium solubility in oxide nuclear fuel. Based on all the experimental data available in the literature and after verification of the validity of Henry's law we propose two correlations for Henry's constant, k_H (at m^{-3} MPa^{-1}):

$k_H = 1.\,8{\cdot}10^{25}\exp(-0.\,41/kT)$ for powders and

$k_H = 4.1{\cdot}10^{24}\exp(-0.\,65/kT)$ for single crystals,

with the Boltzmann factor 1/kT in (eV^{-1}). The correlation for Henry's constant in powder samples is of interest for the analysis of helium behaviour in the fuel after the pulverization occurring during LOCA-like temperature transients, while the correlation for Henry's constant in single-crystals is usable in meso-scale models describing helium behaviour at the level of fuel grains. The current lack of data for this fundamental property, especially for poly-crystalline samples, calls for new experiments.

1. Introduction

An accurate knowledge of helium behaviour is fundamental for evaluating the nuclear fuel performance both in operating and in storage conditions. After production by ternary fissions, (n, α)-reactions and α-decay (Botazzoli, 2011; Federici et al., 2007), helium is either released from the fuel, increasing the fuel rod internal pressure, or retained in the fuel. In the latter case, the behaviour of helium and the other inert gases produced by fissions (xenon and krypton) within the matrix of nuclear fuel grains can be considered as a two-step process (Olander, 1976; Matzke, 1980). The first step is the formation of a population of intra-granular bubbles, exchanging gas with the matrix through the trapping and the re-solution mechanisms (absorption into bubbles and release from the bubbles into the matrix, respectively). The second process is the diffusion of single gas atoms generated in the fuel grains towards the grain boundaries. At the grain boundaries, the inflow of the fission gas atoms, which is controlled by the diffusivity and the solubility, leads to the growth of inter-granular bubbles, whose interconnection contributes to the fission gas release. The volume occupied by both intra- and inter-granular bubbles contributes to the gaseous swelling of the fuel (White and Tucker, 1983; Van Uffelen, 2002; Pastore et al., 2018; Barani et al., 2017; Pizzocri et al., 2018).

In general, helium is used as filling gas (typically at a pressure of 20 bars) in the fuel rods of light water reactors (LWRs). During the first several months of operation, helium initially loaded in the fuel rod free volume can be absorbed into UO_2 (Vinjamuri and Owen, 1980) (this process depending on the helium pressure, on the fuel temperature and porosity).

Another complex issue to face is represented by the large quantities of helium produced in the spent fuel matrix due to α-decaying actinides (Ferry et al., 2006). In fact, the accumulation of helium linked to α-damage creates bubbles at grain-boundaries, which may affect the spent fuel mechanical properties and could eventually cause loss of grain cohesion, with the ultimate risk of reducing the spent fuel pellet to powder (Sattonnay et al., 2006; Wiss et al., 2014; Eyal and Fleischer, 1985; Poinssot et al., 2005). On the other hand, if helium is released from the spent fuel matrix, it could increase the internal pressure on the cladding (representing the first confinement barrier) and lead to its rupture (Freyss et al., 2006).

Therefore, in view of the crucial role played by helium in nuclear fuel, in the last fifty years several experiments have been performed to investigate its key properties: the diffusivity (Belle, 1961; Rufeh, 1964; Rufeh et al., 1965; Sung, 1967; Trocellier et al., 2003; Guilbert et al., 2004; Roudil et al., 2004; Ronchi and Hiernaut, 1967; Martin et al., 2006; Pipon et al., 2009; Nakajima et al., 2011; Garcia et al., 2012; Talip et al., 2014a; Luzzi et al., 2018) and the solubility (Belle, 1961; Hasko and Szwarc, 1963; Rufeh, 1964; Rufeh et al., 1965; Sung, 1967; Blanpain et al., 2006; Maugeri et al., 2009; Nakajima et al., 2011; Talip et al., 2014b).

In this work, we derive new correlations for helium solubility based on an extensive overview of all the experimental results available in the open literature. The complementary work on helium diffusivity in oxide nuclear fuel has been already addressed in a previous paper (Luzzi et al., 2018). After the verification of the validity of Henry's law for the He-UO_2 system and the classification of the resulting data on the basis of the sample microstructure, we derive empirical correlations for Henry's constant of helium in uranium dioxide.

2. Methodology

In this work, as first step, we have verified that helium solubility in UO_2 systems can be described by Henry's law as reported in Section 4. To this purpose, we have selected a consistent set of experimental data and verified that the solubility is linearly proportional to the pressure at fixed temperature. Secondly, the experimental data available in the open literature have been classified on the basis of the microstructure of

https://doi.org/10.1016/j.nucengdes.2018.09.024
Received 23 April 2018; Received in revised form 5 September 2018; Accepted 21 September 2018

Table 1
Comparison of the helium solubility in UO_2 powder.

Reference	Sample	He infusion pressure (MPa)	Solubility (at m^{-3})	Temperature (K)
Belle (1961)	UO_2 powder (≈0.16 μm)	0.1	$2.13 \cdot 10^{22}$	1073
Hasko and Szwarc (1963)	UO_2 powder	11	$9.91 \cdot 10^{22}$	1073
Bostrom (as reported by Rufeh (1964))	UO_2 powder (≈0.15 μm)	0.1	$6.59 \cdot 10^{22}$	1073
		0.1	$3.08 \cdot 10^{22}$	1273
Rufeh et al. (1965)	UO_2 powder (≈4 μm)	10	$1.81 \cdot 10^{25}$	1473
		5	$4.52 \cdot 10^{24}$	1473
		10	$8.72 \cdot 10^{24}$	1573
Blanpain et al. (2006)	UO_2 powder (≈10 μm)	0.2	$1.26 \cdot 10^{23}$	1273
		0.2	$1.14 \cdot 10^{23}$	1473
		0.2	$1.07 \cdot 10^{23}$	1573

Table 2
Comparison of the helium solubility in UO_2 single crystals.

Reference	Sample	He infusion pressure (MPa)	Solubility (at m^{-3})	Temperature (K)
Hasko and Szwarc (1963)	UO_2 single crystal	11	$1.65 \cdot 10^{22}$	1073
Sung (1967)	UO_2 single crystal (≈1 μm)	4.8	$1.34 \cdot 10^{23}$	1473
		6.9	$2.61 \cdot 10^{23}$	1473
		9.0	$3.35 \cdot 10^{23}$	1473
		4.8	$1.72 \cdot 10^{23}$	1623
		6.9	$3.13 \cdot 10^{23}$	1623
		9.0	$4.05 \cdot 10^{23}$	1623
		4.8	$2.02 \cdot 10^{23}$	1773
		6.9	$4.05 \cdot 10^{23}$	1773
		9.0	$5.83 \cdot 10^{23}$	1773
Blanpain et al. (2006)	UO_2 single crystal (≈10 μm)	0.2	$1.07 \cdot 10^{22}$	1573
Maugeri et al. (2009)	UO_2 single crystal	100	$1.38 \cdot 10^{23}$	1523
		100	$2.16 \cdot 10^{23}$	1743
Nakajima et al. (2011)	UO_2 single crystal (≈18 μm)	90	$1.03 \cdot 10^{25}$	1473
Talip et al. (2014b)	UO_2 single crystal	98.7	$1.99 \cdot 10^{23}$	1500

the measured samples, obtaining two new correlations with limited application scope (as explained in Section 4). In principle, classifications based on different parameters, such as the O/M ratio, the initial porosity and the density of the samples, can also be made. However, not all the studies in literature report the necessary data, making a more elaborate analysis not trivial. In general, in literature several experimental (Belle, 1961; Hasko and Szwarc, 1963; Rufeh, 1964; Rufeh et al., 1965; Sung, 1967; Blanpain et al., 2006; Maugeri et al., 2009; Nakajima et al., 2011; Talip et al., 2014b) and theoretical studies concerning the behaviour of helium in nuclear fuel are available (Olander, 1965; Grimes et al., 1990; Crocombette, 2002; Petit et al., 2003; Garrido et al., 2004; Freyss et al., 2006; Parfitt and Grimes, 2008; Yun et al., 2009; Gryaznov et al., 2010; Yakub et al., 2010; Yakub, 2011; Noirot, 2014). Unfortunately, only few theoretical analyses (Olander, 1965; Yakub et al., 2010; Yakub, 2011; Noirot, 2014) provide a solubility value that is even calculated with very different approaches. For this reason, we have decided to derive the correlations to be implemented in physics-based models only on the basis of experimental data. To minimize the influence of outliers, we have fitted the available experimental data using a robust regression method, namely the least absolute residuals (LAR) procedure (Heiser, 1987). The LAR method finds a curve that minimizes the absolute difference of the residuals, rather than the squared differences. Therefore, extreme values have a lesser influence on the fit.

3. Overview of available data

All the measurements of helium solubility have been performed by infusion and, as discussed in Section 2, have been classified only on the basis of the microstructure. The sample to be infused is kept for a certain infusion time at a fixed helium pressure and temperature. If the infusion time is enough, equilibrium is reached, and the infused helium concentration corresponds to the solubility. Tables 1 and 2 report all the experimental results available in literature.

Helium solubility in uranium dioxide has been also studied theoretically by Olander (1965), Yakub et al. (2010), Yakub (2011), and more recently by Noirot (2014). Olander (1965) derived the helium solubility in UO_2 directly from atomic properties, basing the calculations upon a statistical-mechanical formula which assumes dissolved helium to behave as a simple harmonic oscillator in an interstitial site in the UO_2 lattice. Furthermore, Yakub et al. (2010) and Yakub (2011) performed molecular dynamics (MD) simulations determining the helium solubility in UO_2 as a function of temperature and UO_2 stoichiometry. Two-box MD simulations were performed in a wide range of helium pressures from those achieved in infusion experiments (a few MPa) up to 4 GPa, as reported in Yakub (2011). The comparison of the simulation results for stoichiometric UO_2 with existing measurements shows a good agreement with the experimental data of helium solubility in single crystals and a maximum discrepancy of ± 1% with the correlation for Henry's constant in single crystal proposed in this work. In addition, no essential deviations from the linear dependence of solubility on pressure was found up to around 0.5 GPa. Recently, Noirot (2014) derived the theoretical value for Henry's constant applying to helium in interstitial positions in UO_2 a method devised to calculate the equilibrium concentration of point defects and gas atoms in the vicinity of a bubble in UO_2. Noirot performed the calculations for different incorporation energies of an helium atom in an interstitial position and for different activation energies for the diffusion of helium in UO_2, obtaining consistent results with both the molecular dynamics computation and the experimental data, and with a maximum discrepancy

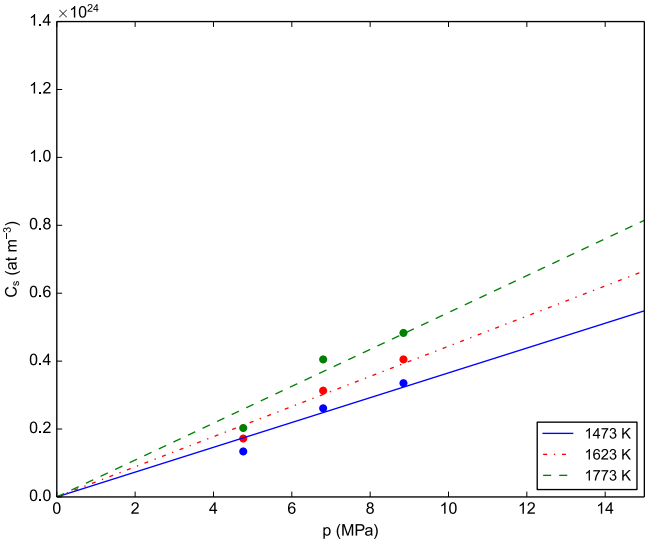

Fig. 1. Comparison of theoretical plot of Henry's law $C_s = k_H\, p$ with experimental results for He-UO_2 system. In detail, the dots are the experimental values for the helium solubility in UO_2 obtained by Sung (1967), while each line represents the linear regression calculated for the data measured at the same temperature.

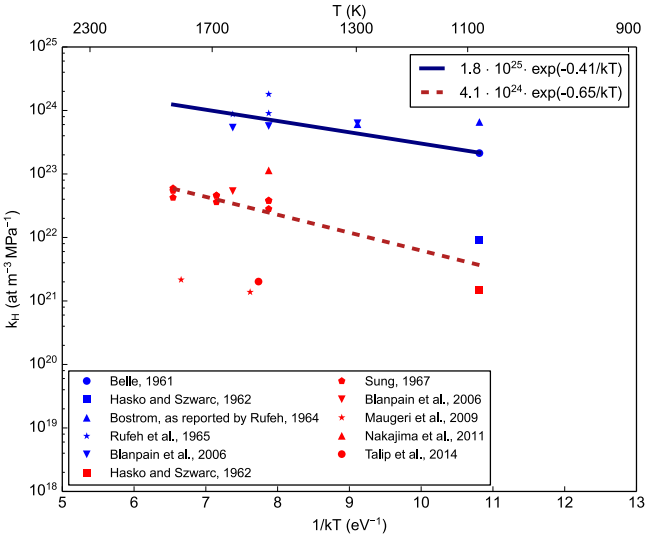

Fig. 2. Plot of the experimental Henry's constant of helium in UO_2 classified depending on the microstructure of the sample (i.e., blue for the powder samples and red for the single crystal samples). Each cluster is fitted by a distinct correlation (bordeaux and blue navy).

of ± 1% with our correlation for single crystals (shown in Section 4).

4. Results and discussion

As shown in Fig. 1, it has been verified that solubility is proportional to infusion pressure and the system He-UO_2 obeys Henry's law (Fig. 1) (Rufeh, 1964; Rufeh et al., 1965; Sung, 1967; Maugeri et al., 2009; Nakajima et al., 2011):

$$C_s = k_H\, p \tag{1}$$

where C_s (at m^{-3}) is the solubility, k_H (at m^{-3} MPa^{-1}) is Henry's constant and p (MPa) is the infusion pressure.

The collected experimental results appear divided in two clusters of data, corresponding to the categorization based on the sample microstructure (Fig. 2). In detail, the cluster in the upper region of the plot includes the powder samples, while the other one in the lower region of the plot includes the single crystal samples.

Despite the large scatter of the experimental results for the helium solubility in uranium dioxide, the resulting clustering of the data (not further critically evaluated here) motivated the derivation of two distinct correlations in the form $k_H = A\, \exp[-B/kT]$. The best estimate correlation for Henry's constant in the powder samples is:

$$k_H = 1.8{\cdot}10^{25} \exp\left(\frac{-0.41}{kT}\right) \tag{2}$$

where k_H (at m^{-3} MPa^{-1}) is Henry's constant, k (eV K^{-1}) the Boltzmann constant and T (K) is the temperature. On the other hand, the best estimate correlation for Henry's constant in the single crystal samples is:

$$k_H = 4.1{\cdot}10^{24} \exp\left(\frac{-0.65}{kT}\right) \tag{3}$$

Table 3 reports the fitting parameters with the related uncertainties[1]

We calculated the uncertainty on the prediction of the solubility by propagating the uncertainty of each fitting parameter. The resulting uncertainty is of the order of a factor of one thousand (×1000) for each correlation herein proposed, while the uncertainty of the fit made

[1] These fitting parameters have been derived applying the LAR (Least Absolute Residuals) method.

Table 3
Summary of the information concerning the fit of correlations. The form is $\mathrm{Log}k_H = \mathrm{Log}A - B/kT\ \mathrm{Log}e$. For each fitting parameter, we report in round brackets the confidence intervals at 95% confidence level.

Data	Log$A$ (at m^{-3} MPa^{-1})	B (eV)	Range (K)	R^2
Powder (Belle, 1961; Hasko and Szwarc, 1963; Rufeh, 1964; Rufeh et al., 1965; Blanpain et al., 2006)	25.25 (23.91, 26.6)	0.41 (0.06, 0.75)	1073–1773	0.83
Single crystal (Hasko and Szwarc, 1963; Sung, 1967; Blanpain et al., 2006; Maugeri et al., 2009; Nakajima et al., 2011; Talip et al., 2014b)	24.61 (23.41, 25.82)	0.65 (0.28, 1.01)	1073–1773	0.83

considering all the data is a factor of ten thousands ($\times$10,000). The proposed categorization therefore allows for a reduction of uncertainties of a factor of ten.

Regarding the applicability, the correlation derived fitting the data concerning the powder samples is usable for the analysis of the helium behaviour in the fuel after the pulverization occurring during LOCA-like temperature transients (Bianco et al., 2015; Cappia, 2017). On the other hand, the correlation proposed for Henry's constant in single crystals is of interest for calculations in meso-scale models dealing with fuel at grain level (like models used in the fuel performance codes for the description of fission gases referring to the fuel grain scale).

Fig. 2 reports all the experimental results analyzed in this work, together with the herein derived correlations for Henry's constant of helium in UO_2. The overall range of temperature covered by the available data is 1073–1773 K.

5. Conclusions

We made an overview of all the experimental results for the helium solubility in UO_2 available in literature. Two clusters emerged based on the microstructure of the measured samples, i.e., powders vs. single crystals. The clustering of the experimental results motivated the derivation of two distinct correlations for Henry's constant as a function of temperature. Recommendations are provided for each new proposed correlation in terms of applicability. This allows obtaining a powder solubility value suitable for describing the helium behaviour in the fuel after his pulverization, and a single crystal solubility value suitable for describing the helium behaviour inside a grain (i.e., for meso-scale models). New experiments would be of great interest, to reduce the uncertainty associated with these correlations and to fill the lack of data concerning the helium solubility in polycrystalline samples with further varying temperatures, oxygen potential and irradiation damage levels. It would be of interest investigating the solubility of helium at higher as well as lower temperatures (for the simulation of nuclear fuel in storage conditions) as more experimental data will become available. Indeed, it would also be interesting to derive a correlation for polycrystalline samples in order to describe the helium behaviour on a macroscopic scale (e.g., in a UO_2 pellet).

Acknowledgments

This work has received funding from the Euratom research and training programme 2014–2018 through the INSPYRE Project under grant agreement No 754329. This research contributes to the Joint Programme on Nuclear Materials (JPNM) of the European Energy Research Alliance (EERA), in the specific framework of the COMBATFUEL Project.

References

Barani, T., Bruschi, E., Pizzocri, D., Pastore, G., Van Uffelen, P., Williamson, R.L., Luzzi, L., 2017. Analysis of transient fission gas behaviour in oxide fuel using BISON and TRANSURANUS. J. Nucl. Mater. 486, 96–110.
Belle, J., 1961. Uranium dioxide: properties and nuclear applications. United States Atom. Energy Commission 569–589.
Bianco, A., Vitanza, C., Seidl, M., Wensauer, A., Faber, W., Macian-Juan, R., 2015. Experimental investigation on the causes for the pellet fragmentation. J. Nucl. Mater. 465, 260–267.
Blanpain, P., Lippens, M., Schut, H., Federov, A.V., Bakker, K., 2006. Helium solubility in UO_2, The HARLEM project. Workshop MMSNF-5, Nice, France.
Botazzoli, P., 2011. Helium production and behaviour in LWR oxide nuclear fuels (Ph.D. thesis). Politecnico di Milano 4–39.
Cappia, F., 2017. Investigation of very high burnup UO_2 fuels in Light Water Reactors (Ph.D. thesis). Technische Universitat Munchen 47–61.
Crocombette, J.-P., 2002. Ab initio energetics of some fission products (Kr, I, Cs, Sr and He) in uranium dioxide. J. Nucl. Mater. 305, 29–36.
Eyal, Y., Fleischer, R.L., 1985. Timescale of natural annealing in radioactive minerals affects retardation of radiation-damage-induced leaching. Nature 314, 518–520.
Federici, E., Courcelle, A., Blanpain, P., Cognon, H., 2007. Helium production and behavior in nuclear oxide fuels during irradiation in LWR. In: Proceedings of the 2007 International LWR Fuel Perfomance Meeting, San Francisco, California. pp. 664–673.
Ferry, C., Poinssot, C., Cappelaere, C., Desgranges, L., Jegou, C., Miserque, F., Piron, J.P., Roudil, D., Gras, J.M., 2006. Specific outcomes of the research on the spent fuel long-term evolution in interim dry storage and deep geological disposal. J. Nucl. Mater. 352, 246–253.
Freyss, M., Vergnet, N., Petit, T., 2006. Ab initio modeling of the behavior of helium and xenon in actinide dioxide nuclear fuels. J. Nucl. Mater. 352, 144–150.
Garcia, P., Martin, G., Desgardin, P., Carlot, G., Sauvage, T., Sabathier, C., Castellier, H., Khodja, H., Barthe, M.F., 2012. A study of helium mobility in polycrystalline uranium dioxide. J. Nucl. Mater. 430, 156–165.
Garrido, F., Nowicki, L., Sattonnay, G., Sauvage, T., Thom, L., 2004. Lattice location of helium in uranium dioxide single crystals. Nucl. Instr. Meth. Phys. Res. Sect. B 219–220, 194–199.
Grimes, R.W., Miller, R.H., Catlow, C.R.A., 1990. The behavior of helium in UO_2: Solution and migration energies. J. Nucl. Mater. 172, 123–125.
Gryaznov, D., Rashkeev, S., Kotomin, E.A., Heifets, E., Zhukovskii, Y., 2010. Helium behavior in oxide nuclear fuels: First principles modeling. Nucl. Instr. Meth. Phys. Res. B 268, 3090–3094.
Guilbert, S., Sauvage, T., Garcia, P., Carlot, G., Barthe, M.F., Desgardin, P., Blondiaux, G., Corbel, C., Piron, J.P., Gras, J.M., 2004. He migration in implanted UO_2 sintered disks. J. Nucl. Mater. 327, 88–96.
Hasko, S., Szwarc, R., 1963. Noble gas solubility and diffusion in UO_2. AEC Division of Reactor Development. Washington.
Heiser, W.J., 1987. Correspondence analysis with least absolute residuals. Comput. Stat. Data Anal. 5, 337–356.
Luzzi, L., Cognini, L., Pizzocri, D., Barani, T., Pastore, G., Schubert, A., Wiss, T., Van Uffelen, P., 2018. Helium diffusivity in oxide nuclear fuel: Critical data analysis and new correlations. Nuclear Eng. Des. 330, 265–271.
Martin, G., Garcia, P., Labrim, H., Sauvage, T., Carlot, G., Desgardin, P., Barthe, M.F., Piron, J.P., 2006. A NRA study of temperature and heavy ion irradiation effects on helium migration in sintered uranium dioxide. J. Nucl. Mater. 357, 198–205.
Matzke, H., 1980. Gas release mechanisms in UO_2 – a critical review. Radiat. Effects 53, 219–242.
Maugeri, E.A., Wiss, T., Hiernaut, J.P., Desai, K., Thiriet, C., Rondinella, V.V., Colle, J.Y., Konings, R.J.M., 2009. Helium solubility and behaviour in uranium dioxide. J. Nucl. Mater. 385, 461–466.
Nakajima, K., Serizawa, H., Shirasu, N., Haga, Y., Arai, Y., 2011. The solubility and diffusion coefficient of helium in uranium dioxide. J. Nucl. Mater. 419, 272–280.
Noirot, L., 2014. A method to calculate equilibrium concentrations of gas and defects in the vicinity of an over-pressured bubble in UO_2. J. Nucl. Mater. 447, 166–178.
Olander, D.R., 1965. Theory of helium dissolution in uranium dioxide. II. Helium solubility. J. Chem. Phys. 43, 785–788.
Olander, D.R., 1976. Fundamental aspects of nuclear reactor fuel elements.
Parfitt, D.C., Grimes, R.W., 2008. Predicted mechanisms for radiation enhanced helium resolution in uranium dioxide. J. Nucl. Mater. 381, 216–222.
Pastore, G., Barani, T., Pizzocri, D., Magni, A., Luzzi, L., 2018. Modelling fission gas release and bubble evolution in UO_2 for engineering fuel rod analysis, accepted contribution for TopFuel2018, Prague, 30.09-04.10.2018.
Petit, T., Freyss, M., Garcia, P., Martin, P., Ripert, M., Crocombette, J.-P., Jollet, F., 2003. Molecular modelling of transmutation fuels and targets. J. Nucl. Mater. 320, 133–137.
Pipon, Y., Raepsaet, C., Roudil, D., Khodja, H., 2009. The use of NRA to study thermal diffusion of helium in (U, Pu)O_2. J. Nucl. Mater. 267, 2250–2254.
Pizzocri, D., Pastore, G., Luzzi, L., Barani, T., Magni, A., Van Uffelen, P., Pitts, S.A., Alfonsi, A., Hales, J.D., 2018. A model describing intra-granular inert gas behavior in oxide fuel for advanced engineering tools. J. Nucl. Mater. 502, 323–330.
Poinssot, C., Ferry, C., Lovera, P., Jegou, C., Gras, J.-M., 2005. Spent fuel radionuclide source term model for assessing spent fuel performance in geological disposal. Part II: matrix alteration model and global performance. J. Nucl. Mater. 346, 66–77.
Ronchi, C., Hiernaut, J.P., 1967. Helium diffusion in uranium and plutonium oxides. J. Nucl. Mater. 325, 1–12.
Roudil, D., Deschanels, X., Trocellier, P., Jégou, C., Peuget, S., Bart, J.M., 2004. Helium

thermal diffusion in a uranium dioxide matrix. J. Nucl. Mater. 325, 148–158.
Rufeh, F., 1964. Solubility of helium in uranium dioxide (M.Sc. thesis). University of California 13–26.
Rufeh, F., Olander, D.R., Pigford, T.H., 1965. The solubility of helium in uranium dioxide. Nucl. Sci. Eng. 23, 335–338.
Sattonnay, G., Vincent, L., Garrido, F., Thom, L., 2006. Xenon versus helium behavior in UO_2 single crystals: a TEM investigation. J. Nucl. Mater. 355, 131–135.
Sung, P., 1967. Equilibrium solubility and diffusivity in single-crystal uranium dioxide (Ph.D. thesis). University of Washington 23–29.
Talip, Z., Wiss, T., Di Marcello, V., Janssen, A., Colle, J.Y., Van Uffelen, P., Raison, P.E., Konings, R.J.M., 2014a. Thermal diffusion of helium in ^{238}Pu-doped UO_2. J. Nucl. Mater. 445, 117–127.
Talip, Z., Wiss, T., Maugeri, E.A., Colle, J.Y., Raison, P.E., Gilabert, E., Ernstberger, M., Staicu, D., Konings, R.J.M., 2014b. Helium behaviour in stoichiometric and hyper-stoichiometric UO_2. J. Eur. Ceram. Soc. 34, 1265–1277.
Trocellier, P., Gosset, D., Simeone, D., Costantini, J.M., Deschanels, X., Roudil, D., Serruys, Y., Grynszpan, R., Saud, S., Beauvy, M., 2003. Application of nuclear reaction geometry for ^{3}He depth profiling in nuclear ceramics. Nucl. Instr. Methods Phys. Res. B 206, 1077–1082.
Van Uffelen, P., 2002. Contribution to the modelling of fission gas release in light water reactor fuel (Ph.D. thesis). Universit de Liege and SCK-CEN 5–34.
Vinjamuri, K., Owen, D.E., 1980. Helium fill gas absorption in pressurized UO_2 fuel rods during irradiation. Nucl. Technol. 47, 119–124.
White, R.J., Tucker, M.O., 1983. A new fission-gas release model. J. Nucl. Mater. 118, 1–38.
Wiss, T., Hiernaut, J.P., Roudil, D., Colle, J.Y., Maugeri, E., Talip, Z., Janssen, A., Rondinella, V.V., Konings, R.J.M., Matzke, H.J., Weber, W.J., 2014. Evolution of spent nuclear fuel in dry storage conditions for millennia and beyond. J. Nucl. Mater. 451, 198–206.
Yakub, E., 2011. Helium solubility in uranium dioxide from molecular dynamics simulations. J. Nucl. Mater. 414, 83–87.
Yakub, E., Ronchi, C., Staicu, D., 2010. Diffusion of helium in non-stoichiometric uranium dioxide. J. Nucl. Mater. 400, 189–195.
Yun, Y., Eriksson, O., Oppeneer, P.M., Kim, H., Park, K., 2009. First-principles theory for helium and xenon diffusion in uranium dioxide. J. Nucl. Mater. 385, 364–367.

L. Cognini[a], D. Pizzocri[a], T. Barani[a], P. Van Uffelen[b], A. Schubert[b], T. Wiss[b], L. Luzzi[a,*]

[a] *Politecnico di Milano, Department of Energy, Nuclear Engineering Division, via La Masa 34, I-20156 Milano, Italy*

[b] *European Commission, Joint Research Centre, Directorate for Nuclear Safety and Security, P.O. Box 2340, 76125 Karlsruhe, Germany*

E-mail address: lelio.luzzi@polimi.it (L. Luzzi)

* Corresponding author.